

## Supporting Information

# Dynamics of Propene and Propane in ZIF-8 Probed by Solid-State $^2\text{H}$ NMR

*Alexander E. Khudozhitkov*<sup>a,b</sup> *Sergei S. Arzumanov*,<sup>a,b</sup> *Daniil I. Kolokolov*,<sup>\*,a,b</sup> *Dieter Freude*,<sup>c</sup>  
*Alexander G. Stepanov*<sup>\*,a</sup>

<sup>a</sup> Borekov Institute of Catalysis, Siberian Branch of Russian Academy of Sciences, Prospekt Akademika Lavrentieva 5, Novosibirsk 630090, Russia

<sup>b</sup> Novosibirsk State University, Pirogova Street 2, Novosibirsk 630090, Russia

<sup>c</sup> Fakultät für Physik und Geowissenschaften, Universität Leipzig, Linnéstr. 5, 04103 Leipzig, Germany

## 1. $^2\text{H}$ NMR spin-lattice and spin-spin relaxation temperature dependences for the perdeuterated propene- $d_6$ .

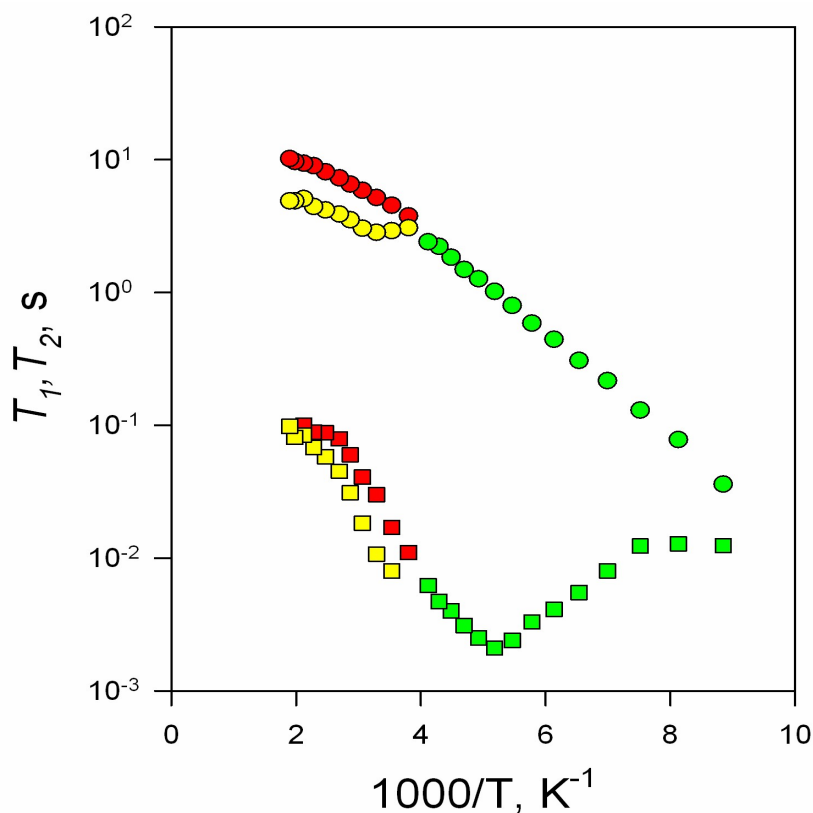


**Figure S1.**  $^2\text{H}$  NMR spin relaxation times  $T_1$  ( $\circ$ ) and  $T_2$  ( $\square$ ) of propene- $d_6$  as a function of the temperature. Relaxation of the unresolved signal is shown in green, of the  $\text{CD}_3$  group is in red, and the relaxation of the  $\text{CD}/\text{CD}_2$  groups (unresolved signal) is in yellow.

## 2. Modeling of spin relaxation

To understand the detailed mechanism of rotations and their kinetic parameters (the activations barriers and rate constants), a detailed fitting analysis of the  $^2\text{H}$  NMR spin relaxation within experimentally studied temperature range is to be performed. Our homemade FORTRAN simulation routines are based on the general formalism proposed by Abragam<sup>1</sup> and developed in details by Spiess<sup>2</sup> and others<sup>3-6</sup>.

Spin relaxation times  $T_1$  and  $T_2$  are generally anisotropic and depend on the observation angles  $\theta$  and  $\varphi$  in the powder pattern. They are given by the usual formula:<sup>2</sup>

$$\frac{1}{T_1} = \frac{3}{4}\pi^2 Q_0^2 (J_1(\omega_0) + 4J_2(2\omega_0)) \quad (1)$$

$$\frac{1}{T_2} = \frac{3}{8}\pi^2 Q_0^2 (3J_0(0) + 5J_1(\omega_0) + 2J_2(2\omega_0)) \quad (2)$$

where the spectral density function  $J_m(\omega)$  for the chosen model of the molecule motion is defined by the expression:

$$J_m(\omega) = 2 \sum_{a,b=-2}^2 D_{a,q}(\Omega_L) * D_{b,q}(\Omega_L) \otimes G_{0,a|0,b}(\omega), \quad (3)$$

where

$$G_{c,a|d,b}(\omega) = \sum_{l,k,n=1}^N D_{c,a}^l(\Omega_l) * D_{d,b}^k(\Omega_k) p_{eq}(l) V_{l,n} \left( \frac{-\lambda_n}{\lambda_n^2 + \omega^2} \right) V_{n,k}^{-1} \quad (4)$$

Here  $\Omega_L$  are the observation angles  $\theta$  and  $\varphi$ , which connect the molecular frame with the laboratory frame;  $\Omega_k$  are the Euler angles which connect the molecular frame with the  $k$ -th distinct position of the  $C-D$  bond within the assumed geometry of the jump model;  $V_{l,n}$  is a matrix composed by Eigen vectors of kinetic matrix  $K$  and  $\lambda_n$  are its Eigen values;  $N$  is the number of distinct jump-sites.

If one or multiple isotropic motions are present the corresponding correlation function is no longer dependent from the polar angles and the resulting function is simply a tensor multiplication of correlation functions for distinct motional modes:

$$J_m(\omega) = 2 \sum_{\substack{a,b=-2 \\ c,d}}^2 D_{a,q}(\Omega_L) * D_{b,q}(\Omega_L) \otimes G_{c,a|d,b}^1(\omega) \otimes G_{0,c|0,d}^2(\omega) \quad (5)$$

Once the individual motional model is defined, the exchange between the states **I** and **II** is modeled as standard chemical exchange of the individual relaxation rates ( $T_1^I$  and  $T_1^{II}$ ) and ( $T_2^I$  and  $T_2^{II}$ ) with respective populations and the exchange rate. The resulting *effective* relaxation times were directly computed from the Bloch's equations:

$$\frac{d}{dt} \begin{pmatrix} M_Z^I \\ M_Z^{II} \end{pmatrix} = \begin{pmatrix} -\frac{1}{T_1^I} - K_{eq} \cdot k_{ex} & K_{eq} \cdot k_{ex} \\ k_{ex} & -\frac{1}{T_1^{II}} - k_{ex} \end{pmatrix} \begin{pmatrix} M_Z^I \\ M_Z^{II} \end{pmatrix} \quad (6)$$

$$\frac{d}{dt} \begin{pmatrix} M_{\perp}^I \\ M_{\perp}^{II} \end{pmatrix} = \begin{pmatrix} -\frac{1}{T_2^I} - K_{eq} \cdot k_{ex} & K_{eq} \cdot k_{ex} \\ k_{ex} & -\frac{1}{T_2^{II}} - k_{ex} \end{pmatrix} \begin{pmatrix} M_{\perp}^I \\ M_{\perp}^{II} \end{pmatrix} \quad (7)$$

where  $M_Z^I$  and  $M_{\perp}^I$  are the longitudinal and transverse magnetization of state **I** and  $M_Z^{II}$  and  $M_{\perp}^{II}$  are corresponding magnetization of state **II**,  $k_{ex}$  is the exchange rate,  $K_{eq} = p_{II}/p_I$  is the equilibrium constant. The effective relaxation  $T_1$  and  $T_2$  are then determined by numerical calculation as Eigenvalues of the exchange matrices.<sup>7</sup> The net longitudinal magnetization decays in biexponential manner with rates equal to eigenvalues of the matrix. Both eigenvalues are negative. One eigenvalue has large magnitude and equal to the  $\lambda_{max} = -k_{ex}(K_{eq} + 1)$  in the fast

exchange limit. The other eigenvalue  $\lambda_{min}$  has low magnitude and contains information about the molecular mobility even in the fast limit. Since  $e^{-\lambda_{max}t}$  decays too fast to be observed in the experiment, the final relaxation rate is chosen as the  $\lambda_{min}$ .

### 3. Synthesis and characterization of the ZIF-8

The material was the same used earlier in ref.<sup>8</sup> for benzene mobility characterization in ZIF-8. It was synthesized following the route reported by Cravillon *et al.*<sup>9</sup> and Keser Demir *et al.*<sup>10</sup> A solution of the  $Zn(NO_3)_2 \cdot 6H_2O$  (2.3 g, Sigma-Aldrich) in 75 mL of MeOH was quickly poured into a solution of 2-miM (5 g) in 75 mL of MeOH under stirring at room temperature with pH mediated by NaOH. After 1h the nanoparticles were separated from the mother solution by centrifugation. The resulting white crystals were washed twice by 100 mL of deionized water (18 h in total) and twice by 100 mL of MeOH (24 h in total). The resulting product was dried under a flush of nitrogen at room temperature and activated at high vacuum at 373 K for 10 h.

The XRD analysis of the activated material (Figure S2) revealed a pattern matching with previously reported data<sup>9, 10</sup>. The X-Ray diffraction patterns were collected on the Siemens D500 instrument using  $CuK\alpha$  radiation. The  $N_2$  adsorption measurement of the activated at 423 K material has shown a BET surface area of  $S_{BET} \sim 1350 \text{ m}^2/\text{g}$  (Figures S3,S4).

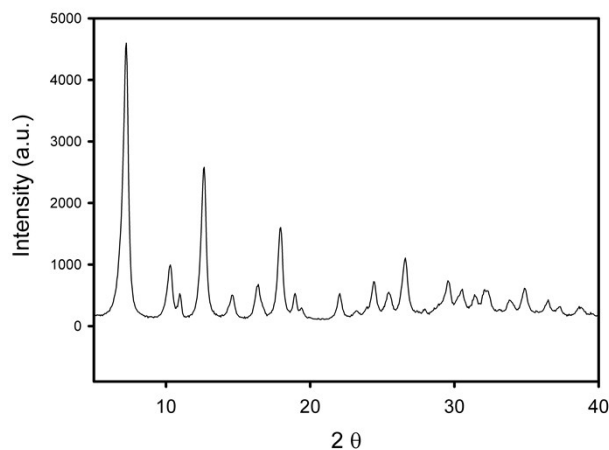


**Figure S2.** XRD pattern of the activated ZIF-8 material. The XRD is the typical fingerprint of ZIF-8 structure.

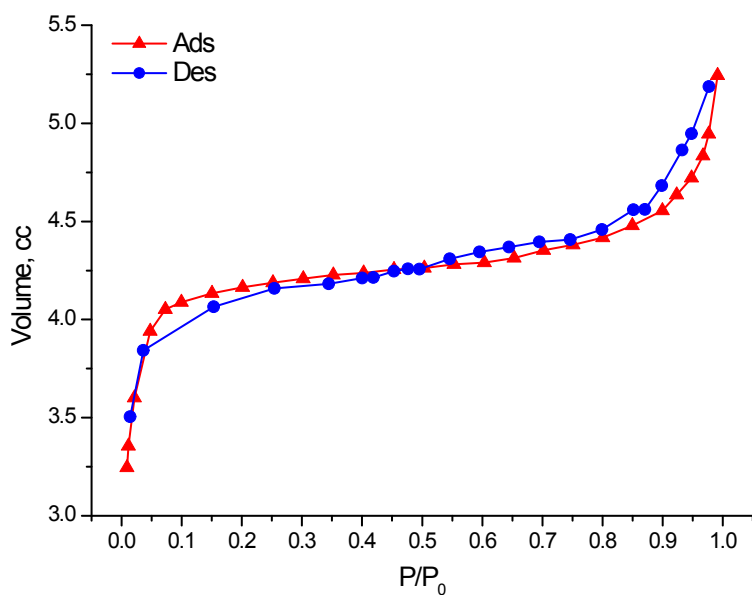


**Figure S3.** Nitrogen adsorption isotherm for the activated ZIF-8.

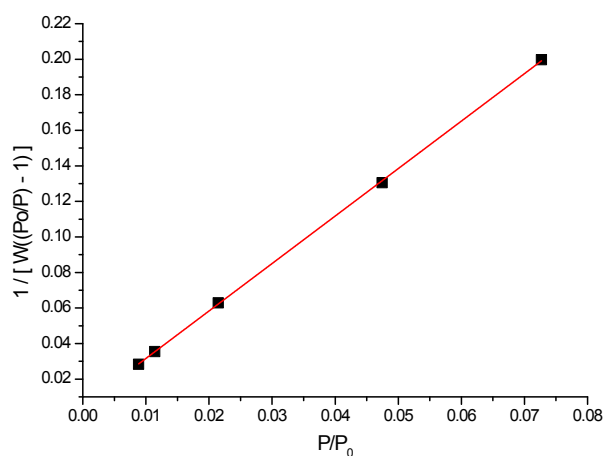


**Figure S4.** Initial adsorption step affords a good linear approximation using the BET model yielding a surface area of  $S_{\text{BET}} \sim 1350 \text{ m}^2/\text{g}$ .

Scanning Electron Microscopy showed regular shaped crystals of uniform distribution.

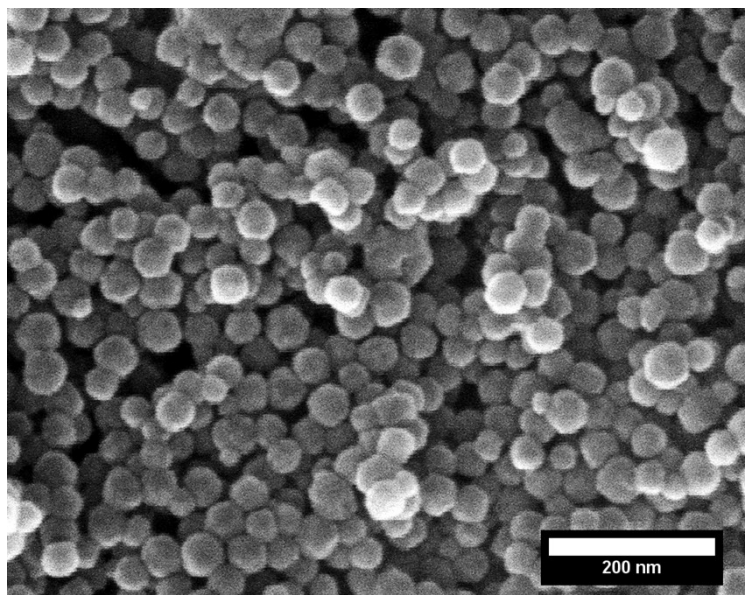


**Figure S5.** SEM image of the synthesized ZIF-8 particles. The images were taken on a JEOL JSM-6700F instrument (acceleration voltage = 5 kV, current = 10  $\mu$ A).

#### References:

1. A. Abragam, *The Principles of Nuclear Magnetism*, Oxford University Press, Oxford, UK, 1961.
2. H. W. Spiess, in *NMR Basic Principles and Progress*, eds. P. Diehl, E. Fluck and R. Kosfeld, Springer-Verlag, New York, 1978, vol. 15, p. 55–214.
3. R. J. Wittebort and A. Szabo, *J. Chem. Phys.*, 1978, **69**, 1722–1736.
4. R. J. Wittebort, E. T. Olejniczak and R. G. Griffin, *J. Chem. Phys.*, 1987, **86**, 5411–5420.
5. G. Lipari and A. Szabo, *Biophys. J.*, 1980, **30**, 489–506.
6. L. J. Schwartz, E. Meirovitch, J. A. Ripmeester and J. H. Freed, *J. Phys. Chem.*, 1983, **87**, 4453–4467.
7. D. I. Kolokolov, A. G. Maryasov, J. Ollivier, D. Freude, J. Haase, A. G. Stepanov and H. Jobic, *J. Phys. Chem. C*, 2017, **121**, 2844–2857.
8. D. I. Kolokolov, L. Diestel, J. Caro, D. Freude and A. G. Stepanov, *J. Phys. Chem. C*, 2014, **118**, 12873–12879.
9. J. Cravillon, S. Munzer, S. J. Lohmeier, A. Feldhoff, K. Huber and M. Wiebcke, *Chem. Mater.*, 2009, **21**, 1410–1412.
10. N. Keser Demir, B. Topuz, L. Yilmaz and H. Kalipcilar, *Microporous Mesoporous Mater.*, 2014, **198**, 291–300.